Physics of Fluids

LETTER | FEBRUARY 20 2024

Mixing dynamics in the synthesis of nanoparticle-stabilized water-in-water emulsion: Impact on size and stability

Chandra Shekhar ; Vishal Singh Pawak ; Vishwajeet Mehandia ; Sashikumar Ramamirtham ; Monicka Kullappan ; Manigandan Sabapathy

Physics of Fluids 36, 021703 (2024)
https://doi.org/10.1063/5.0187697

Physics of Fluids LETTER pubs.aip.org/aip/pof

Mixing dynamics in the synthesis of nanoparticle-stabilized water-in-water emulsion: Impact on size and stability

Cite as: Phys. Fluids **36**, 021703 (2024); doi: 10.1063/5.0187697
Submitted: 15 November 2023 · Accepted: 21 January 2024 ·
Published Online: 20 February 2024

Chandra Shekhar,[1] Vishal Singh Pawak,[1] Vishwajeet Mehandia,[1] Sashikumar Ramamirtham,[2] Monicka Kullappan,[3,a)] and Manigandan Sabapathy[1,a)]

AFFILIATIONS

[1]Department of Chemical Engineering, Indian Institute of Technology Ropar, Rupnagar 140001, India
[2]Edinburgh Complex Fluids Partnership, The University of Edinburgh, Edinburgh EH9 3FD, United Kingdom
[3]GE Research, Niskayuna, New York 12309, USA

[a)]**Authors to whom correspondence should be addressed:** monickakullappan@gmail.com and mani@iitrpr.ac.in

ABSTRACT

This communication presents a comprehensive investigation into the impact of mixing on the synthesis of water-in-water Pickering emulsions. The approach employs commercial-grade oppositely charged nanoparticles within two distinct fluid phases, facilitating self-assembly and the formation of aggregates with variable sizes and compositions. Enhanced interfacial area, achieved through aggregate adsorption at the interface, elevates the Gibbs detachment energy of particles between the two aqueous phases, leading to stable emulsion formation. We further explore the effect of various mixing devices, including high-pressure and sonic wave mixing. Our findings reveal that mixing within the aqueous phase critically influences emulsion size, with sonicator-assisted mixing producing smaller droplets than homogenizer mixing. Both devices yield poly-dispersed droplet size distributions. Interestingly, the droplet size correlates well with the Hinze scale (h_d), and the Kolmogorov length scale (l_d) exhibits good correspondence within a specific operating range. The proposed method introduces a streamlined, one-step synthesis process for easy preparation, demonstrating excellent stability for a minimum of 30 days. This study pioneers the investigation of mixing effects within an aqueous two-phase system utilizing a Pickering emulsion template.

Complex fluids refer to a class of materials characterized by the presence of internal microstructures, and their evolution significantly influences the macroscopic dynamics of the materials. This category encompasses various substances, such as polymers and melts, liquid crystals, gels, suspensions, emulsions, and micellar solutions.[1] These materials hold substantial practical significance as their microstructure can be intentionally manipulated during processing, resulting in favorable mechanical, optical, and thermal properties. One effective strategy for harnessing the potential of complex fluids is developing composites. By amalgamating two immiscible components and adjusting parameters such as composition, concentration, phase morphology, and mixing behavior, it becomes possible to generate composites with novel and enhanced properties.[2] The current investigation focuses exclusively on emulsions produced via an aqueous two-phase system (ATPS), particularly emphasizing the water-in-water (w/w) emulsion. The primary emphasis is on complex fluids, including Pickering emulsions; the utilization of ATPS via emulsion formation highlights the adaptability of complex fluid systems. Therefore, this study contributes to the broader field of complex fluid dynamics by focusing on Pickering emulsions formed using ATPS.

Aqueous two-phase systems (ATPSs) represent thermodynamically balanced systems achieved by amalgamating two incompatible hydrophilic polymers into two distinct phases. An archetypal illustration of ATPS is the water-in-water (W/W) emulsion, wherein two hydrophilic macromolecules engender a heterogeneous amalgam of aqueous phases, with one phase dispersed in the form of droplets within the other. Contemporary advancements in emulsion droplet generation techniques have engendered a plethora of applications across a spectrum of domains encompassing drug delivery, food industries, cosmetics, emulsion explosives, and reaction media.[3,4] The interfacial tension between these aqueous phases in this particular emulsion category is profoundly feeble, typically spanning the range of 1–10 μN/m. This subdued interfacial tension is an outcome of the analogous chemical constitution of the two aqueous phases, thereby yielding enfeebled

intermolecular forces and minimal thermodynamic hindrances at the interface. The position of the tie-line in a biphasic diagram is influenced by the volumes of the phases chosen along the binodal diagram. We employed a binodal curve to identify the thermodynamic state of two-phase regions, wherein the systems chosen at specific operating regime phase separate spontaneously. The binodal curve distinguishes a region of component concentrations leading to the formation of two immiscible aqueous phases (above the curve) from those resulting in a single phase (at and below the curve), as reported in our previous work elsewhere.[5] It is important to note that the placement of the tie-line is also dependent on the concentrations of both polymers and as a result, the interfacial tension can vary accordingly.[6] It is noteworthy that selecting concentrations for phase separation that significantly deviate from the binodal curve along the same tie-line may not lead to substantial change in interfacial tension. Subsequently, the oppositely charged nanoparticles (OCNPs) have been utilized as emulsifiers to stabilize the w/w emulsion droplets formed as a result of emulsifying the ATPS. The interaction between particles at the interface refers to the forces and phenomena influencing the arrangement and behavior of colloidal particles at the boundary between different phases. These interactions, often dominated by intermolecular forces, are essential for maintaining stability against coalescence, preventing the merging or aggregation of particles.[7,8] The distinctive attributes inherent to ATPS, including biocompatibility, modifiable selectivity, and mild processing requisites, have galvanized their integration in diverse applications encompassing bioseparation, biocatalysis, and drug delivery.[5,6,9]

The preparation of emulsions can be accomplished using various mechanical emulsification techniques, such as membrane systems, high-pressure systems, ultrasonic systems, and rotor-stator systems (e.g., disk systems or Ultraturrax). The resulting droplet size distributions can vary based on process conditions, including energy input, phase viscosities, type of disk, or interfacial influencing parameters (such as emulsifier type and concentration).[10] For instance, the average size of droplets inversely varies with the rate of energy input raised to the power 0.4 per Kolmogorov scale as given in the following equation:[11]

$$a \approx E^{-0.4}\gamma^{0.6}\rho^{-0.2}, \tag{1}$$

where E, γ, and ρ are the rate of energy per unit volume, interfacial tension at the fluid–fluid interface, and density of the continuous medium, respectively. However, in the water-in-water (w/w) emulsion, the morphologies are less influenced by mixing energy.[5,12] The low interfacial tension between both phases simplifies emulsion stabilization, achievable through straightforward handshaking.

Urban *et al.*, Gómez *et al.*, and Calvo *et al.* have investigated the impact of different parameters on cosmetic emulsions. They explored factors such as phase concentration, energy input, and stability. These studies demonstrated that altering these parameters during emulsion synthesis can change the droplet size and texture. Enhanced stability was observed with decreased droplet size resulting from high-pressure mixing. The influence of mixing conditions on macroscopic properties can be more pronounced depending on the dispersed phase concentration. This phenomenon is linked to heightened interactions between droplets at the microscopic level. Furthermore, the research indicates that tip velocity and impeller pumping capacity are valuable factors for up-scaling emulsification. Adjusting these parameters can significantly affect energy consumption, drop deformation, and breakage.[13–15]

While the existing body of literature is robust, recent scientific investigations have demonstrated that colloidal particles of diverse compositions exhibit the ability to accumulate at interfaces between water phases. These particles encompass solid spherical entities such as silica, polystyrene, and proteins as well as microorganisms, anisotropic clay particles, cellulose nanorods, deformable microgel particles, and protein-stabilized emulsion droplets.[16–23] Achieving effective stabilization of water–water (W/W) emulsions through particle-based mechanisms necessitates the establishment of a state characterized by close-packing and/or aggregation of colloidal particles at the water–water interface. This results in the formation of a robust interfacial barrier surrounding the dispersed water droplets, offering resistance against coalescence and macroscopic phase separation.[9] There remains a discernible dearth of studies scrutinizing the ramifications of mixing in the context of water–water (W/W) emulsion synthesis.[5,24–26]

This article addresses this research gap, shedding light on the relatively unexplored realm of mixing energy effects in the fabrication of W/W emulsions, their droplet size, stability, and delineates potential trajectories for future investigations in this promising domain.

Our approach utilizes mechanical and acoustic energy to generate water-in-water (w/w) emulsions. This methodology employs polyethylene oxide (PEO), dextran bio-compatible and bio-polymer, respectively, and oppositely charged silica nanoparticles to induce *in situ* hetero-aggregate formation within an aqueous phase to achieve the longer stability of the stabilized emulsion. The focal point of this study revolves around examining the repercussions of energy interplay during emulsion synthesis within aqueous two-phase systems (ATPSs). The outcomes of our investigation underscore the potential of our unified and streamlined approach for the scalable and proficient fabrication of w/w emulsions characterized by robust stability. For the synthesis of w/w emulsions, we utilize polyethylene oxide (PEO) and dextran biopolymers having molecular weights: 1×10^5 (1e5) and 4×10^4 (4e4) Da, respectively. Our experimental strategy incorporates Ludox HS-40 (40 wt%) and CL-30 (30 wt%) silica nanoparticles, boasting a diameter of 16 ± 2 nm as ascertained through transmission electron microscopy (Fig. S1), and zeta potentials of -55 ± 1.8 and 51 ± 2.1 mV, respectively, as determined by electrophoretic light scattering.

Figure 1 depicts a schematic representation of the emulsion preparation process. Each phase was synthesized independently by homogenizing with varying weight fractions of PEO ranging from 1% to 7% and dextran from 3% to 9% of the total solution. These fractions are denoted as λ, representing the ratio of the percentage fraction of dextran to the percentage fraction of PEO. Both mixtures were allowed to soak overnight at room temperature and subjected to 2 min of vortex mixing to prepare a homogeneous polymer solution. Following this, each particle (CL-30 with PEO or HS-40 with dextran solution) was mixed into one of the phases so that the total concentration of the nanoparticles did not exceed 1 wt. % in the entire solution. The two suspensions were combined in a sample vial and thoroughly mixed using a homogenizer (IKA, Model: Ultra Turrax T25) or a probe-type sonicator (Branson, Model: SFX 250) operating at various speeds or amplitudes for 2 min. After mixing, the samples were incubated at a constant temperature of 25 °C for 48 h. Deionized water (18.2 MΩ), obtained from the Barnstead™ Smart2Pure™ water purification system (Make: Thermo Fisher Scientific), was used for all sample preparations. Notably, all samples were examined after 48 h, serving as the

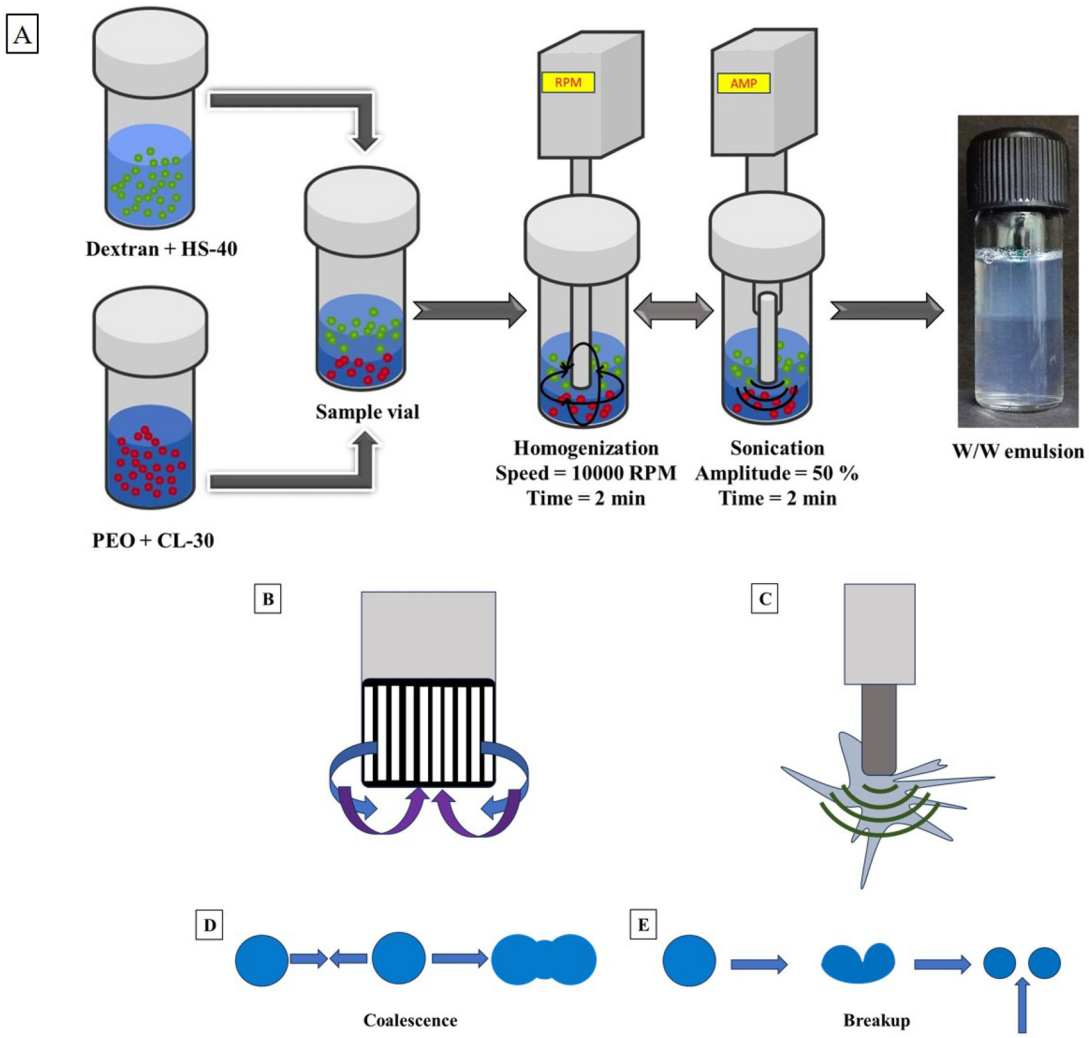

FIG. 1. Schematic description of the emulsion formation using different mixing devices.

reference point (t = 0 days) for comparative analysis. All experiments were conducted in triplicate to ensure the reliability and repeatability of the results. The volume fraction of the phases exhibiting two-phase formation has been previously discussed in our earlier article published elsewhere.[5]

First, we propose an approach for synthesizing water-in-water (w/w) emulsions utilizing a Pickering template with oppositely charged nanoparticles (OCNPs). This article aims to investigate the impact of mixing energy on the synthesis of w/w emulsions, employing both high-pressure mixing and ultrasonic sound energy. Our methodology involves preparing an aqueous phase incorporating bio-polymers while carefully selecting a specific weight ratio of positively charged nanoparticles to negatively charged nanoparticles, denoted as "M." This approach enables the creation of a w/w Pickering emulsion template.

The proposed study presents a comprehensive investigation to assess the impact of various process parameters within the Pickering emulsion system, originally designed for oil-in-water (o/w) emulsions, as outlined in Tsabet and Fradette.[27] An essential parameter we scrutinized was the mixing process, given its critical role in emulsion synthesis. Specifically, we employed ultrasonication for the nanoemulsion synthesis within an oil–water system, in line with the approaches described in Ramisetty *et al.*[28] and Ghosh *et al.*[29] Our investigation has unveiled that increasing the mixing energy applied during the emulsification of w/w emulsions results in the growth of the droplet size in the resulting emulsion. This observed phenomenon is commonly referred to as "over-processing," and it arises due to the occurrence of re-coalescence within the emulsion droplets.[30–34] The emulsification process comprises two distinct steps: (1) the deformation and disruption of droplets, resulting in an increase in the specific surface area of the emulsion, and (2) the stabilization of this newly created interface through the use of an emulsifier, which serves to prevent the re-coalescence of the freshly formed droplets. Newly formed droplets are inherently thermodynamically unstable, except in the case of micro-emulsions, primarily due to incomplete interface coverage by emulsifier

molecules. In the interim, between the formation of new droplets and their subsequent interaction with surrounding droplets, emulsifiers adsorb onto the emerging interface, effectively preventing re-coalescence. If the timescale required for emulsifiers' absorption is greater than the timescale of collision between droplets, the emulsifiers added may only partially cover the newly formed interface. Consequently, this incomplete coverage of the fresh interface can result in re-coalescence. This intriguing phenomenon implies that even when the energy input during emulsification is elevated, the resulting emulsions may exhibit larger droplet sizes than anticipated, contrary to the expected outcome of achieving smaller droplet sizes.[35] Several factors influence the droplet size and re-coalescence within emulsions. These factors encompass the emulsifier's efficacy, the energy input level during the emulsification process, the dispersed phase's concentration, the emulsion's viscosity, and the temperature conditions.

Our research significantly advances our comprehension of the roles played by emulsifiers and energy inputs in synthesizing water-in-water emulsions. Within aqueous two-phase systems (ATPSs), where a relatively low surface tension ($\approx 10^{-6}$–10^{-7} N/m) exists between the phases, creating emulsions for practical applications poses a notable challenge. The Gibbs detachment energy equation (ΔG_d), as outlined in Eq. (2), indicates that the low interfacial tension results in lower detachment energy, implying weak emulsion stability. The lowered stability is because the energy required to pull or detach particles from the droplet surface becomes very small. To overcome this challenge, compensatory measures are needed. One strategy involves employing larger-sized particles to increase the interfacial area ($A_{fluid-fluid}$) and, consequently, the Gibbs detachment energy. Alternatively, we utilize oppositely charged nanoparticles to induce self-assembly, forming aggregates of varying sizes more significant than the individual nanoparticles. This approach allows us to raise the detachment energy and achieve water-in-water emulsions with the desired stability, which can be further tuned by the concentration of nanoparticles, the ratio of weight fraction of positively charged to negatively charged nanoparticles and the molecular weight of the polymers employed in the respective aqueous phases. Our group has previously reported studies related to this methodology in the literature.[5,12,24]

$$\Delta G_d = \pi r^2 \gamma_{w-w} (1 \pm \cos\theta)^2, \tag{2}$$

where γ_{w-w}, r, and θ refer to interfacial tension between water–water interface, radius of a particle, and the three phase contact angle, respectively.

To explore the influence of emulsification devices and their energy input on stabilizing water-in-water (w/w) emulsions, our study leveraged anisotropic particles, specifically hetero-aggregates formed by oppositely charged nanoparticles (OCNPs). Through a methodical approach, we systematically varied the polymer concentration and the M ratio (defined as the ratio of positively charged nanoparticles to the negatively charged counterparts) within the system. This deliberate manipulation resulted in observable changes in the droplet size of the emulsions we synthesized. These observations provided valuable insights into the impact of these factors on the structural characteristics and stability of the emulsions under investigation. Notably, our analysis was exclusively focused on the characterization of droplets per the state diagram reported by our group earlier. However, the emergence of a bicontinuous network structure indicates the formation of two-dimensional hierarchical architectures akin to bicontinuous jammed emulsions (bijels). This distinctive structure manifests when the wettability established by the given stabilizer at the water–water interface is equally probable when the contact angle (θ) is approximately 90° and the volume fraction employed is 50%. The intricate clusters (M) formed at the interface contribute to the development of bijels, and the arrangement of these clusters is influenced by the presence of free particles in the vicinity of the interface. The availability of these free particles tends to alter the arrangement of aggregates at the interface due to attraction and repulsion forces, thereby impacting the contact angle of the aggregates which favors the bijel formation in the w/w emulsion.[5] Based on our experimental observations, we have formulated a state diagram illustrating the droplet size stabilization achieved by OCNPs when employing a homogenizer and a sonicator, both operated at a desired speed and amplitude of 10 000 rpm and 50%, respectively, for 2 min. This state diagram is depicted in Fig. 2. In Fig. 2(a), we present the droplet sizes synthesized using the two different mixing devices. In contrast, in Fig. 2(b), we provide the corresponding standard error (%) for these droplet sizes. These state diagrams are valuable tools for selecting the optimal combination of polymer and particle concentrations that result in the smallest droplets and the lowest standard deviation.

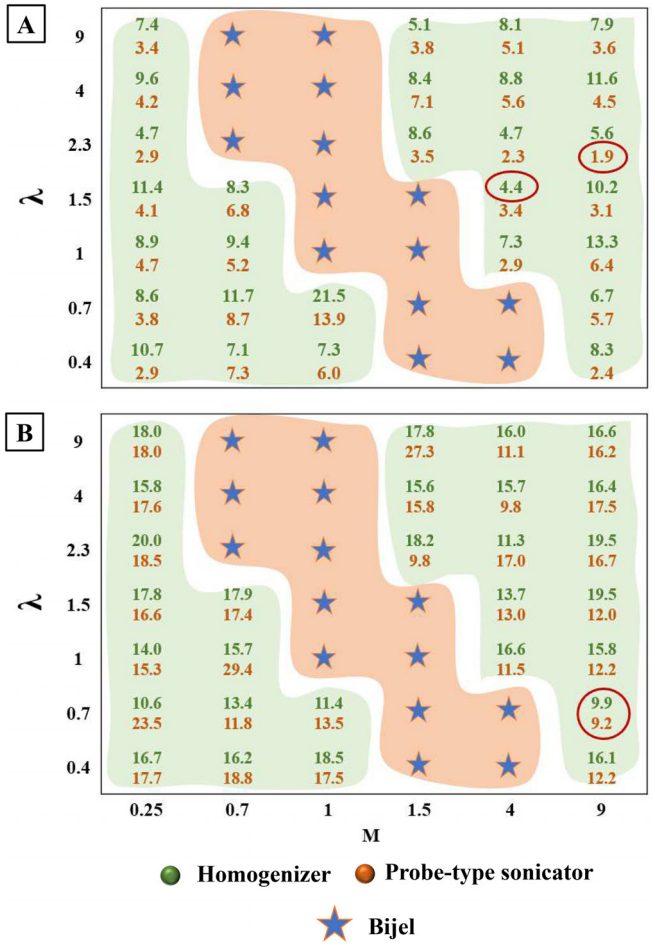

FIG. 2. State diagram demonstrating (a) droplet size and (b) percentage standard error of the formed droplets with respect to the polymer concentration and M.

Figure S2 displays the drop images captured using an inverted microscope (Model: Axio Vert A1; Make: Carl Zeiss, India) in brightfield mode. The images were captured at a magnification of 40× to provide a broader view of the sample's surface area and visually depict the emulsion's stability over time. The samples were prepared by depositing them carefully on cleaned glass slides and covered with coverslip to prevent solvent evaporation. These images enable the assessment of changes in emulsion morphology, including variations in the droplet size, shape, and distribution. Such data are essential for gauging emulsion stability and evaluating the effectiveness of the stabilizing agents employed in the system. The size distribution of the droplets formed was determined from the microscopic images, as illustrated in Fig. S3.

Single-charged particles have demonstrated the capability to stabilize the emulsion; nevertheless, our research group has reported issues regarding the overall stability of the emulsion elsewhere.[5] Based on the state diagram we constructed for various mixing devices, it has been observed that at a polymer concentration of 7% dextran and 3% PEO, with an M value of 9, the droplet size is significantly smaller compared to other compositions. Conversely, when utilizing a homogenizer, the composition of 6% dextran and 4% PEO with an M value of 4 yields the smallest droplets. This trend suggests that an M value of 9 is critical for achieving smaller emulsion droplets when employing a sonicator. However, it is worth noting that further investigation into sub-micron/nano water-in-water (w/w) emulsion is warranted using a bulk synthesis approach.

We have constructed an energy diagram for both mixing devices, which is correlated with the mixing speed (rpm) and amplitude frequency (%) applied during the emulsion mixing process. This energy diagram is depicted in Fig. 3, and it serves as a representation of the energy input applied to the system during the emulsification process. To investigate the impact of the mixing process, we selected the composition with the smallest droplet size, which consists of 7% dextran and 3% PEO at an M value of 9, wherein we employed a mixing speed of 10 000 rpm and amplitude frequency of 50% for comparison purposes. Initially, our investigation focused on the impact of mixing on the size of hetero-aggregates for both devices at these specified speeds and amplitudes. Figure S4 illustrates that increasing the mixing energy forms smaller clusters when using both devices. However, clusters mixed with the sonicator exhibit approximately half the size compared to those mixed with the homogenizer. This difference is a significant factor contributing to the formation of smaller-sized droplets. We have also measured the size of the clusters formed at M = 9 at the different amplitudes of the mixing in polymer and water to understand the effect of energy to modify the aggregate size. Figure 4 shows that the size of particle aggregates in the polymer solutions remains nearly constant beyond a critical sonication amplitude, mirroring the trend in pure water. This suggests that the increase in the droplet size at higher applied energy levels is attributed to over-processing within the system.

Furthermore, we investigated the emulsification process using the previously selected composition (7% dextran and 3% PEO, M = 9) at various mixing speeds and amplitude while maintaining a constant mixing duration of 2 min for effective stabilization. This approach aligns with the findings of Tsabet and Fradette. They reported that increasing the mixing time beyond a certain threshold does not significantly impact the droplet size under optimal conditions.[27]

Figure 5 illustrates how mixing affects emulsion droplet size. It reveals three distinct zones, one indicating consistent droplet sizes at optimal speeds and the other portraying the consequences of over-processing, diffusive (homogenization), or cavitation (sonication) during emulsification. In Fig. 5(a), representing the homogenizer, the initial increase in the droplet size can be attributed to diffusion phenomena during the mixing process. As the emulsion is initiated under the influence of elevated shear through the application of a high-pressure homogenizer under turbulent flow conditions, optimal droplet breakup occurs, leading to the attainment of minimal droplet size.[36] Subsequent increases in the droplet size under heightened shear conditions are attributed to molecular diffusion, specifically the Ostwald ripening process.[37] Ostwald ripening entails the growth of larger droplets within an emulsion at the expense of smaller droplets, facilitated by

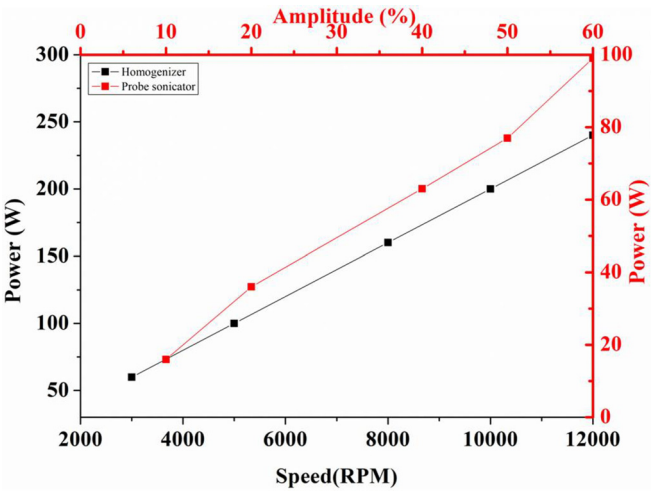

FIG. 3. Power as a function of speed and amplitude of the different devices.

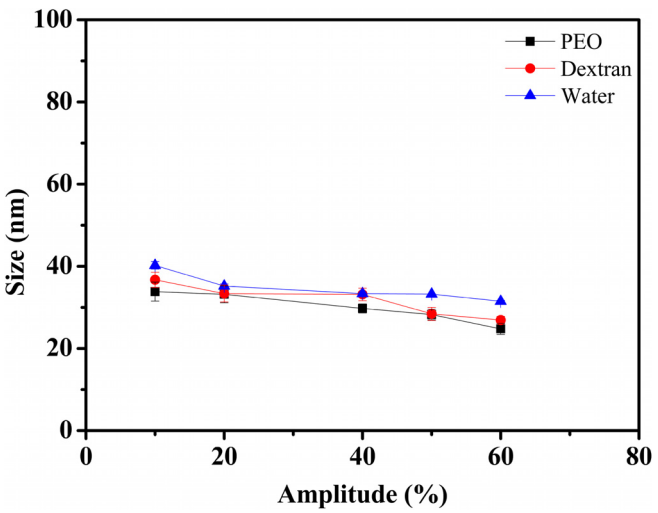

FIG. 4. Size of aggregates formed at M = 9 at different amplitude of the mixing in polymer and water medium.

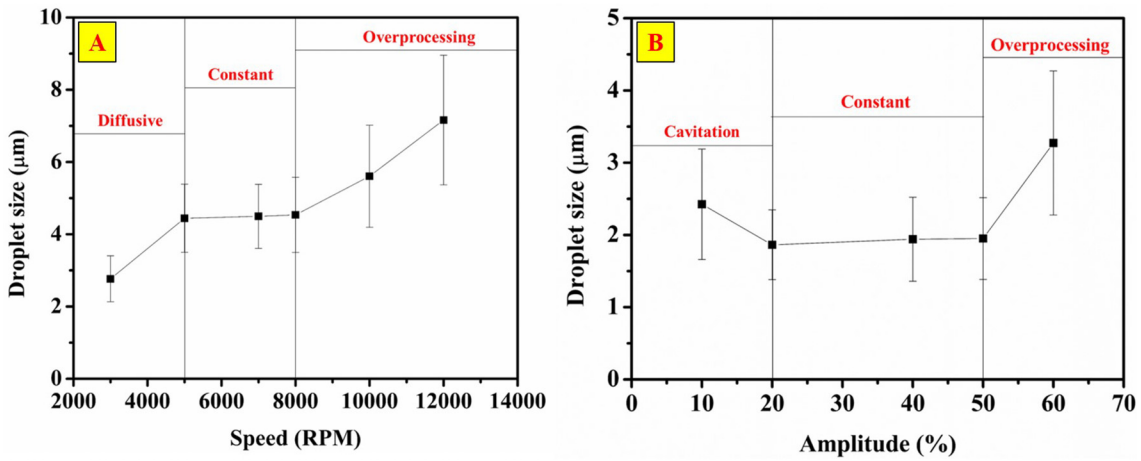

FIG. 5. Mixing effect on droplet size with 7% dextran and 3% PEO at M = 9.

the molecular diffusion between droplets through the continuous phase.[8,37] However, as the speed is elevated from 5000 to 8000 rpm, there is no further alteration in the droplet size, signifying that this range represents the optimal mixing speed for achieving the desired droplet size. Beyond this range, with further increases in speed, there is a continuous escalation in the droplet size due to over-processing in the system. Figure 5(b), which pertains to the sonicator, demonstrates a different trend. Initially, there is a decrease in the droplet size, which can be attributed to the high cavitation effect on the initial droplets formed, causing them to break into smaller sizes. Further increasing the sonication power up to 50% amplitude has minimal impact on droplet size and results in nearly constant droplets. However, when sonication amplitude is further increased, it leads to over-processing in the solution, resulting in the formation of larger-sized droplets due to re-coalescence among the initially formed droplets. Figure 6 presents microscopic images of the droplets formed using various

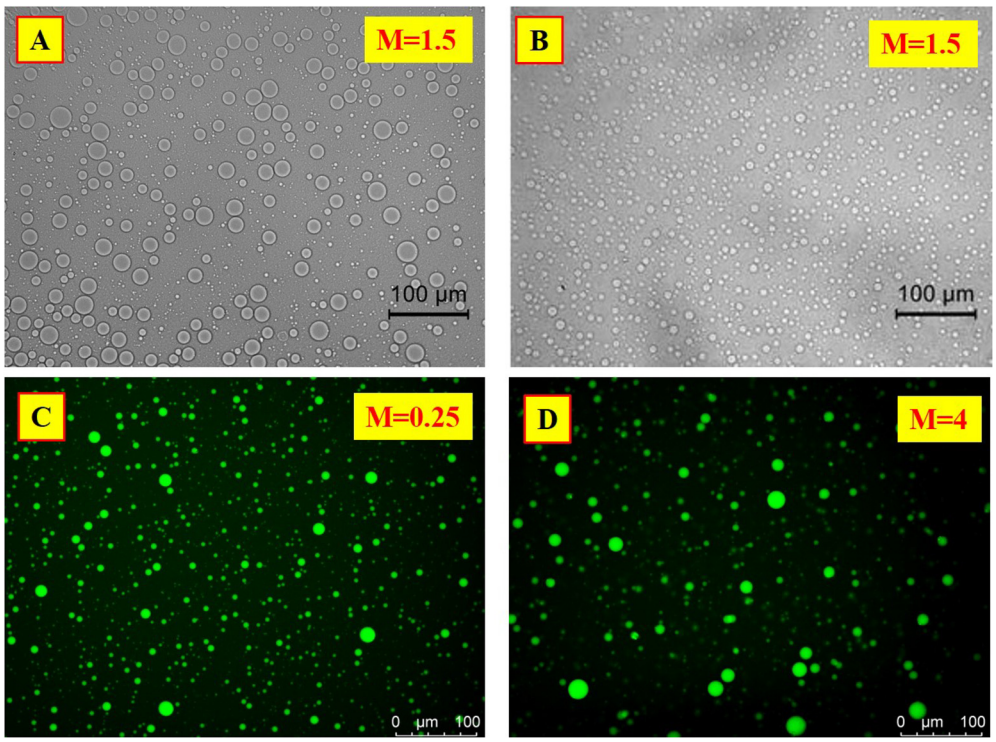

FIG. 6. Microscopic insights: (a) and (b) Comparative micrographs of the samples emulsified using homogenizer and sonicator, respectively, at $\lambda = 2.3$. (c) and (d) Fluorescent micrographs of dextran-in-PEO droplets stabilized using homogenizer corresponding to the mixing ratio (λ) of 0.4 at M = 0.25 and 4, respectively. The scale bar corresponds to the 100 μm.

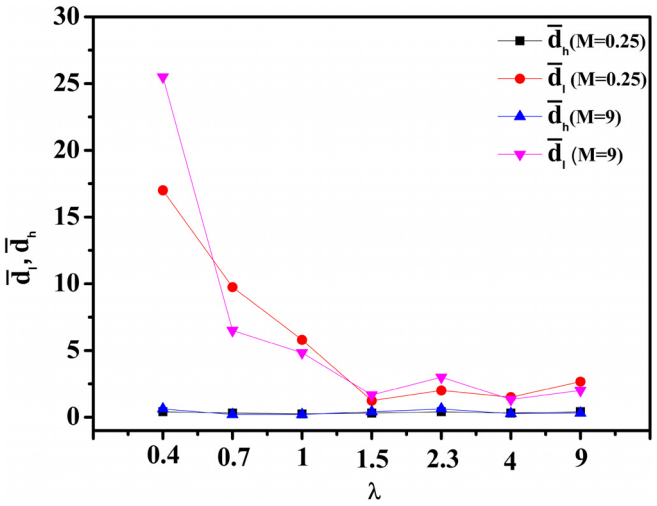

FIG. 7. Comparison of Kolmogorov (l_d) and Hinze (h_d) scale (H) analysis with the experimental values at M = 0.25 and 9.

emulsification devices under different mixing conditions. These images visually depict the alterations in the droplet size. It can be inferred from Fig. 6(b) that the emulsification performed using the probe-type sonicator yields droplets with minimal average diameter when λ is 2.3. Figures 6(c) and 6(d) reveal the structural morphology of the droplets distinctly at different M values.

It is intriguing to note that the type of deformation and breakup depends not only on the physical properties of the two phases but also on the flow field imposed on the droplets. Per the study conducted by Hinze, we understand that the type of flow induced by the homogenizer and sonicator could cause the "type 1" deformation due to turbulent flow conditions and the varying contacting patterns that could be linked to axisymmetric hyperbolic or rotating flow field, respectively.[38] Figure 7 presents the Kolmogorov length scale and droplet size as a function of the mass ratio (λ) of dextran to PEO. The Kolmogorov length scale (l_d) and Hinze scale (h_d) diameter are defined as follows:

$$l_d = \left((\eta/\rho)^3/\varepsilon\right)^{1/4}, \tag{3}$$

$$h_d = \mathrm{We}_c \left(\frac{\sigma}{\rho_c}\right)^{3/5} \varepsilon^{-2/5}, \tag{4}$$

where We_c, η, ρ, σ, and ε are referred to as critical Weber number, viscosity, density, interfacial tension, and energy dissipation or power input per unit mass, respectively. The critical Weber number (We_c) given in Eq. (4) is calculated by the following relation as reported by Hinze:[38]

$$(N_{We})_c = \frac{\rho \bar{v}^2 D_{max}}{\sigma}. \tag{5}$$

Since the droplets are smaller than the smallest eddies (l_d) and the viscous stresses dominate over inertial stresses, the equation proposed by Shinnar[39] could be employed to compute the local velocity gradient ($\bar{v}$) which is a function of the energy dissipation and kinematic viscosity, while the correlation proposed by Hinze is used to determine the largest drop size (D_{max}).[38]

$$\bar{v}^2 = (\varepsilon\eta/\rho)^{1/4}, \tag{6}$$

$$D_{max} = \frac{0.725}{\rho_c^{3/5}\varepsilon^{2/5}} \times \sigma^{3/5}. \tag{7}$$

Furthermore, we have rescaled the droplet diameter using the predicted diameter, as defined by Hinze and Kolmogorov [Eqs. (8) and (9)]. The rescaled diameter of the droplet approaches values slightly less than or close to 1, indicating that the Hinze scale agrees well with the experimental values.

$$\bar{d}_h = \frac{D_{Hinze}(h_d)}{D_{experimental}}, \tag{8}$$

$$\bar{d}_l = \frac{D_{Kolmogorov}(l_d)}{D_{experimental}}. \tag{9}$$

Referring to Fig. 7, it can be stated that the constancy over the droplet size for a particular λ ranging between 1.5 and 9 could be achieved when a probe-type sonicator is employed. The average droplet size measured correlates well with l_d, when λ is 1.5–9 and is within one order magnitude difference. On the other hand, the droplet size measured over a broad range of λ is in good agreement with the Hinze scale approximation for both M values. It is worth noting that the M values chosen at 0.25 and 9 enable us to analyze the droplet diameter in the whole range of λ. A quick analysis of droplet size vs a Kolmogorov length scale (l_d) could indicate that the mechanism of droplet breakup prevails when a sonicator is being used as an emulsification device, as shown in Fig. 1(e). To understand the effect of phases in the formed emulsion droplet and their stability, we have chosen the emulsion formed using 3% dextran and 7% PEO, resulting in a D/P-type emulsion. We contrasted this with an altered concentration, specifically 7% dextran and 3% PEO, forming a P/D-type emulsion corresponding to the tie-line of both phases. For the D/P-type emulsion at M = 0.25, the size of the formed droplets is almost double

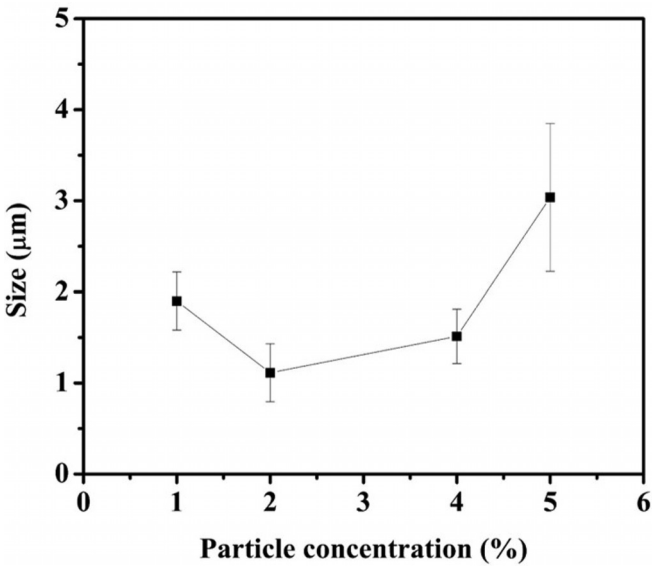

FIG. 8. The impact of total particle concentration (wt.%) on droplet size under optimum sonication conditions.

when using a homogenizer compared to a sonicator along the P/D-type emulsion. However, there is no change in the droplet size when the emulsion is prepared using sonication in both types of emulsions. At M = 9, the droplet size in the P/D-type emulsion is smaller using both devices, as illustrated in Fig. 2. The smaller droplet size in the P/D-type emulsion at M = 9 suggests a more stable emulsion. Nevertheless, the stability in both types of emulsions remains constant, as demonstrated in Fig. 9, indicating stable emulsions for up to 60 days. Furthermore, our investigation delved into the influence of particle concentration on emulsion formation. Optimal sonication conditions were maintained with a 50% amplitude at $\lambda = 2.3$ and M = 9. Various total particle concentrations (1, 2, 4, and 5 wt. %) were employed consistently under these sonication conditions. Our findings revealed that elevating the total particle concentration within the system led to the attainment of an optimal particle concentration, resulting in the smallest droplet size observed at 2 wt. %, as depicted in Fig. 8. Subsequent increments in concentration increased droplet size, potentially attributed to the formation of larger aggregates within the system.

The stability of the formed emulsion was evaluated over a 60-day period. Emulsion stability was quantified by calculating the emulsion index (%), which was determined using Eq. (10),[40] and inferring the Fig. 9. This assessment was carried out for various mass ratios (M) of nanoparticles using the vial images presented in Fig. S5.

$$EI = \frac{h}{H} \times 100. \tag{10}$$

Here, h and H denote the height of the emulsion phase and the total sample height, respectively. To calculate this index, we determined the percentage ratio of the emulsion height (the vertical extent covered by the emulsion) to the overall height of the mixture after emulsification. This measurement was conducted using the Image-J software, an open-source software tool. The results indicated that emulsions formed with single particles, such as HS-40 and CL-30, in this system could stabilize the emulsion with very low stability. A quick overview of the state of formed emulsions at different M can be obtained by referring to the vial images in Fig. S5.

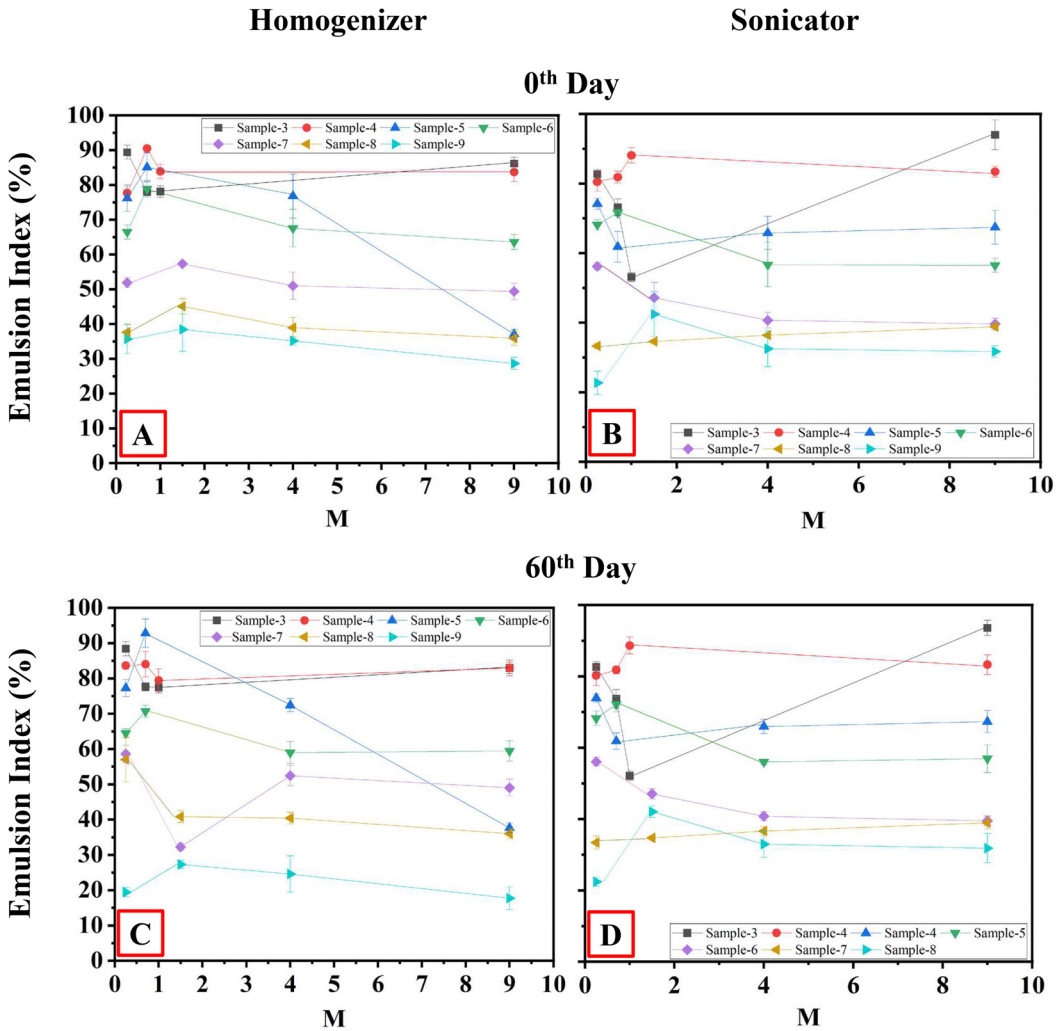

FIG. 9. Plot showing the stability of the formed emulsion.

In this work, we have demonstrated the synthesis of colloidal capsules utilizing various emulsification techniques within a water-in-water Pickering emulsion system. We employed oppositely charged nanoparticles to stabilize the emulsion in the form of aggregates or clusters. We conducted a comparative analysis of droplet sizes by utilizing two distinct emulsification methods: mechanical agitation and low-power ultrasound (sonication at 20 kHz) using both a homogenizer and a sonicator employing a probe-type micro-tip. We investigated the influence of different power inputs on the system, using the concentration of dextran and PEO as key components, on the size of the resulting capsules. Subsequently, we constructed a state diagram to illustrate the average diameter of the droplets produced by both processes (see Fig. 2). The diagram indicates that smaller droplets were formed when an amplitude of 50% (equivalent to 77 W) and a polymer concentration of 7% dextran + 3% PEO with an M value of 9 was applied.

Additionally, we constructed a corresponding state diagram for the deviation of the droplet size resulting from the different devices. The variability in % standard error is attributed to changes in aggregate size at varying M values. These state diagrams represent the pivotal findings of our study, providing valuable insights into the selection of specific polymer concentrations and M values based on desired droplet size and standard deviation criteria. Furthermore, we generated frequency distribution curves corresponding to droplet size at different M values and polymer concentrations. Moreover, we have demonstrated that the emulsions produced through sonication (see Fig. 9) exhibit outstanding stability, exceeding 60 days. In contrast, the stability of the emulsion achieved with the homogenizer (as depicted in Fig. 9) is somewhat lower at approximately 45 days. This lower stability is primarily attributed to the larger droplet size resulting from the operation at 10 000 rpm (200 W). It is important to note that the larger droplet size can contribute to destabilization, primarily due to sedimentation phenomena within the emulsion. Since our technique relies on stabilizing the droplets through the self-assembly[41–43] of oppositely charged nanoparticles, the necessary increase in Gibbs detachment energy occurs naturally without the need for the addition of unconventional stabilizers. This study marks the first comprehensive exploration of the impact of energy input on the synthesis of water-in-water (W/W) emulsions using a Pickering emulsion template within an aqueous two-phase system (ATPS) through a streamlined, single-step process.

SUPPLEMENTARY MATERIAL

See the supplementary material for transmission electron microscopic images of OCNPs, microscopic images of the formed emulsion, droplet size distribution, size of aggregates formed using OCNPs using different devices, and vial images of the formed emulsion.

ACKNOWLEDGMENTS

We gratefully acknowledge financial support from the Core Research Grant (No. CRG/2022/005880) sponsored by the Science and Engineering Research Board (SERB), India. We thank Dr. Swati A. Patel, Department of Chemical Engineering, Indian Institute of Technology Ropar, for extending support to access the probe-type sonicator.

AUTHOR DECLARATIONS

Conflict of Interest

The authors have no conflicts to disclose.

Author Contributions

Chandra Shekhar: Data curation (equal); Formal analysis (equal); Investigation (equal); Methodology (equal); Writing – original draft (equal). **Vishal Singh Pawak:** Data curation (equal); Formal analysis (equal); Investigation (equal); Methodology (equal); Writing – original draft (equal). **Vishwajeet Mehandia:** Formal analysis (supporting); Investigation (supporting); Validation (supporting). **Sashikumar Ramamirtham:** Formal analysis (supporting); Investigation (supporting); Validation (supporting). **Monicka Kullappan:** Formal analysis (equal); Investigation (equal); Validation (equal); Writing – review & editing (equal). **Manigandan Sabapathy:** Conceptualization (equal); Formal analysis (equal); Investigation (equal); Project administration (equal); Resources (equal); Supervision (equal); Writing – review & editing (equal).

DATA AVAILABILITY

The data that support the findings of this study are available from the corresponding authors upon reasonable request.

REFERENCES

[1]M. Kröger and J. Vermant, *The Structure and Rheology of Complex Fluids* (Oxford University Press, 2000).
[2]P. Yue, J. J. Feng, C. Liu, and J. Shen, "A diffuse-interface method for simulating two-phase flows of complex fluids," J. Fluid Mech. **515**, 293–317 (2004).
[3]J. Esquena, "Water-in-water (W/W) emulsions," Curr. Opin. Colloid Interface Sci. **25**, 109–119 (2016).
[4]W. J. Frith, "Mixed biopolymer aqueous solutions – Phase behaviour and rheology," Adv. Colloid Interface Sci. **161**, 48–60 (2010).
[5]C. Shekhar, A. Kiran, V. Mehandia, V. R. Dugyala, and M. Sabapathy, "Droplet–bijel–droplet transition in aqueous two-phase systems stabilized by oppositely charged nanoparticles: A simple pathway to fabricate bijels," Langmuir **37**, 7055–7066 (2021).
[6]T. Nicolai and B. Murray, "Particle stabilized water in water emulsions," Food Hydrocolloids **68**, 157–163 (2017).
[7]L. Tea, F. Renou, L. Benyahia, and T. Nicolaï, "Assessment of the stability of water in water emulsions using analytical centrifugation," Colloids Surf. A: Physicochem. Eng. Aspects **608**, 125619 (2021).
[8]T. J. Wooster, M. Golding, and P. Sanguansri, "Impact of oil type on nanoemulsion formation and Ostwald ripening stability," Langmuir **24**, 12758–12765 (2008).
[9]E. Dickinson, "Particle-based stabilization of water-in-water emulsions containing mixed biopolymers," Trends Food Sci. Technol. **83**, 31–40 (2019).
[10]O. S. El Kinawy, S. Petersen, L. Helmdach, and J. Ulrich, "Parameter selection of emulsification processes: conditions for nano- and macroemulsions," Chem. Eng. Technol. **35**, 1604–1608 (2012).
[11]E. Dickinson, *An Introduction to Food Colloids* (Oxford University Press, Oxford, 1992).
[12]C. Shekhar, V. Mehandia, and M. Sabapathy, "Single-step generation of double emulsions in aqueous two-phase systems," Phys. Fluids **35**, 073109 (2023).
[13]K. Urban, G. Wagner, D. Schaffner, D. Röglin, and J. Ulrich, "Rotor-stator and disc systems for emulsification processes," Chem. Eng. Technol. **29**, 24–31 (2006).
[14]I. Gómez, F. Calvo, J. M. Gómez, L. Ricardez-Sandoval, and O. Alvarez, "A multiscale approach for the integrated design of emulsified cosmetic products," Chem. Eng. Sci. **251**, 117493 (2022).
[15]F. Calvo, J. M. Gómez, O. Alvarez, and L. Ricardez-Sandoval, "Effect of emulsification parameters on the rheology, texture, and physical stability of cosmetic emulsions: A multiscale approach," Chem. Eng. Res. Des. **186**, 407–415 (2022).
[16]B. P. Binks, "Particles as surfactants—Similarities and differences," Curr. Opin. Colloid Interface Sci. **7**, 21–41 (2002).
[17]E. Dickinson, "Food emulsions and foams: Stabilization by particles," Curr. Opin. Colloid Interface Sci. **15**, 40–49 (2010).

[18]H. Firoozmand and D. Rousseau, "Tailoring the morphology and rheology of phase-separated biopolymer gels using microbial cells as structure modifiers," Food Hydrocolloids **42**, 204–214 (2014).
[19]M. Vis, J. Opdam, I. S. Van't Oor, G. Soligno, R. Van Roij, R. H. Tromp, and B. H. Erné, "Water-in-water emulsions stabilized by nanoplates," ACS Macro Lett. **4**, 965–968 (2015).
[20]W. J. Ganley, P. T. Ryan, and J. S. van Duijneveldt, "Stabilisation of water-in-water emulsions by montmorillonite platelets," J. Colloid Interface Sci. **505**, 139–147 (2017).
[21]K. R. Peddireddy, T. Nicolai, L. Benyahia, and I. Capron, "Stabilization of water-in-water emulsions by nanorods," ACS Macro Lett. **5**, 283–286 (2016).
[22]E. Ben Ayed, R. Cochereau, C. Dechanceé, I. Capron, T. Nicolai, and L. Benyahia, "Water-in-water emulsion gels stabilized by cellulose nanocrystals," Langmuir **34**, 6887–6893 (2018).
[23]C. Griffith and H. Daigle, "On the shear stability of water-in-water Pickering emulsions stabilized with silica nanoparticles," J. Colloid Interface Sci. **532**, 83–91 (2018).
[24]C. Shekhar, S. G. Marapureddy, V. Mehandia, V. R. Dugyala, and M. Sabapathy, "Probing emulsion-gel transition in aqueous two-phase systems stabilized by charged nanoparticles: A simple pathway to fabricate water-in-water emulsion-filled gels," Colloids Surf. A: Physicochem. Eng. Aspects **670**, 131474 (2023).
[25]W. Cui, C. Xia, S. Xu, X. Ye, Y. Wu, S. Cheng, R. Zhang, C. Zhang, and Z. Miao, "Water-in-water emulsions stabilized by self-assembled chitosan colloidal particles," Carbohydr. Polym. **303**, 120466 (2023).
[26]S. Yan, J. M. Regenstein, S. Zhang, Y. Huang, B. Qi, and Y. Li, "Edible particle-stabilized water-in-water emulsions: Stabilization mechanisms, particle types, interfacial design, and practical applications," Food Hydrocolloids **140**, 108665 (2023).
[27]E. Tsabet and L. Fradette, "Effect of processing parameters on the production of pickering emulsions," Ind. Eng. Chem. Res. **54**, 2227–2236 (2015).
[28]K. A. Ramisetty, A. B. Pandit, and P. R. Gogate, "Ultrasound assisted preparation of emulsion of coconut oil in water: Understanding the effect of operating parameters and comparison of reactor designs," Chem. Eng. Process.: Process Intensification **88**, 70–77 (2015).
[29]V. Ghosh, A. Mukherjee, and N. Chandrasekaran, "Ultrasonic emulsification of food-grade nanoemulsion formulation and evaluation of its bactericidal activity," Ultrason. Sonochem. **20**, 338–344 (2013).
[30]E. Tornberg, "Functional characteristics of protein stabilized emulsions: Emulsifying behavior of proteins in a sonifier," J. Food Sci. **45**, 1662–1668 (1980).
[31]M. B. Schulz and R. Daniels, "Hydroxypropylmethylcellulose (HPMC) as emulsifier for submicron emulsions: Influence of molecular weight and substitution type on the droplet size after high-pressure homogenization," Eur. J. Pharm. Biopharm. **49**, 231–236 (2000).
[32]G. Kolb, K. Viardot, G. Wagner, and J. Ulrich, "Evaluation of a new high-pressure dispersion unit (HPN) for emulsification," Chem. Eng. Technol. **24**, 293–296 (2001).
[33]P. Marie, J. Perrier-Cornet, and P. Gervais, "Influence of major parameters in emulsification mechanisms using a high-pressure jet," J. Food Eng. **53**, 43–51 (2002).
[34]S. M. Jafari, Y. He, and B. Bhandari, "Production of sub-micron emulsions by ultrasound and microfluidization techniques," J. Food Eng. **82**, 478–488 (2007).
[35]S. M. Jafari, E. Assadpoor, Y. He, and B. Bhandari, "Re-coalescence of emulsion droplets during high-energy emulsification," Food Hydrocolloids **22**, 1191–1202 (2008).
[36]P. W. Voorhees, "Ostwald ripening of two-phase mixtures," Annu. Rev. Mater. Sci. **22**, 197–215 (1992).
[37]T. Tadros, P. Izquierdo, J. Esquena, and C. Solans, "Formation and stability of nano-emulsions," Adv. Colloid Interface Sci. **108–109**, 303–318 (2004).
[38]J. O. Hinze, "Fundamentals of the hydrodynamic mechanism of splitting in dispersion processes," AIChE J. **1**, 289–295 (1955).
[39]R. Shinnar, "On the behaviour of liquid dispersions in mixing vessels," J. Fluid Mech. **10**, 259–275 (1961).
[40]F. Shahaliyan, A. Safahieh, and H. Abyar, "Evaluation of emulsification index in marine bacteria Pseudomonas sp. and Bacillus sp," Arab. J. Sci. Eng. **40**, 1849–1854 (2015).
[41]Y. Shelke, M. Sabapathy, and E. Mani, "Staggered linear assembly of spherical-cap colloids," Langmuir **33**, 6760–6768 (2017).
[42]M. Sabapathy, Y. Shelke, M. G. Basavaraj, and E. Mani, "Synthesis of non-spherical patchy particles at fluid–fluid interfaces via differential deformation and their self-assembly," Soft Matter **12**, 5950–5958 (2016).
[43]M. Sabapathy, S. D. Christdoss Pushpam, M. G. Basavaraj, and E. Mani, "Synthesis of single and multipatch particles by dip-coating method and self-assembly thereof," Langmuir **31**, 1255–1261 (2015).